Systematic Investigations on the Influence of Viscosity Index Improvers on EHL Film Thickness

Bernd-Robert Höhn, Klaus Michaelis and Franz Kopatsch

Nomenclature

A	deformed area of disk capacitor
C	capacitance of disk capacitor
C	thermal correction factor acc. Murch/Wilson (Ref. 12)
E_1, E_2	Young's modulus of contact bodies
E'	reduced Young's modulus
F_N	normal force
G	EHL-parameter of elasticity
L	thermal load factor acc. Murch/Wilson (Ref. 12)
M_w	weight average molecular weight
P	polymer correction factor
R	reduced radius of curvature
SSI	shear stability index
U	EHL parameter of velocity
VI	viscosity index
W	EHL parameter of load
b	deformed Hertzian contact width
d_a	tip circle
d_b	base circle
d_w	pitch circle
f	frequency of resonance circuit
h_{meas}	measured lubricant film thickness
h_{min}	minimum film thickness calculated acc. Dowson/Higginson (Ref. 5)
h_0	film thickness in the parallel gap calculated acc. Ertel/Grubin (Refs. 6 and 8)
l_{eff}	disk width
p_H	Hertzian contact pressure
r_1, r_2	radius of curvature of contact bodies
s	slip ratio ($s = 1 - v_2/v_1$)
v_1, v_2	surface velocity of contact bodies ($v_2 < v_1$)
v_Σ	hydrodynamic velocity ($v_\Sigma = v_1 + v_2$)
α	pressure-viscosity coefficient
α_t	temperature coefficient of dynamic viscosity
γ	shear rate
ε_{oil}	relative dielectric coefficient of the oil
ε_0	electric field constant ($\varepsilon_0 = 8.8542 \cdot 10^{-12}\ C/(Vm)$)
η	dynamic viscosity
η_M	dynamic viscosity at bulk temperature
ϑ	temperature
ϑ_M	average bulk temperature ($\vartheta_M = (\vartheta_1 + \vartheta_2)/2$)
ϑ_1, ϑ_2	bulk temperature of contact bodies
ϑ_{oil}	oil inlet temperature
λ	heat conductivity of lubricant (mineral oil: $\lambda \approx 0.133\ W/(m \cdot K)$)
ν	kinematic viscosity
ν_1, ν_2	Poisson's ratio of contact bodies
ω	angle velocity

Printed with permission of the copyright holder, the American Gear Manufacturers Association, 1500 King Street, Suite 201, Alexandria, Virginia 22314. Copies of the paper are available from the association.

Introduction

Mineral-oil-base lubricants show a significant decrease of kinematic viscosity with rising temperature, as exemplified in Figure 1 by lubricants for vehicle gears. An important attribute of lubricants is their viscosity index (VI), according to DIN/ISO 2909 (Ref. 4). Viscosity index is a calculated coefficient, which characterizes the change of viscosity of lubricants as a function of temperature. A high viscosity index represents a low variation of viscosity due to temperature and vice versa. A low viscosity-temperature-dependence is required for lubricants that are operated at significantly varying temperature conditions, such as vehicle engine and gear lubricants in summer and winter time. This way, the oils remain flowing and pumpable at low temperatures on the one hand; and on the other hand, sufficiently thick lubricant films can be formed at higher temperatures for a safe separation of the surfaces.

A deliberate improvement of the viscosity temperature behavior can be achieved by blending an oil with polymer additives as viscosity-index improvers, such as polyalkylmethacrylate (PMA), olefin copolymer (OCP), styrene butadiene copolymer (SBC) or polyisobutylene (PIB). This way, polymer-free monograde oils can be converted into multigrade oils, which are used in large quantities as engine oils in vehicles (e.g. SAE 15W-40), as gear oils in manual transmissions in vehicles (e.g. SAE 75W-90, see Fig. 1) or in automatic transmissions (e.g. ATF DEXRON® type oils). Universal oils for tractors and earth-movers (e.g. UTTO), which can be used for hydraulics and gears, are multigrade oils as well.

The viscosity-increasing effect of polymer additives at laboratory conditions is known and can be proved. However, their efficiency at EHL conditions of high pressure, high shear rate and high temperature, such as in gear or roller-bearing contacts, is questionable. Polymer-containing oils can suffer from a temporary viscosity loss by high shear rates in an EHL contact, and they can suffer from a permanent viscosity loss by a partial mechanical destruction of the polymers during operation. That results in a lower operating viscosity and, hence, worse lubricating conditions than one would expect according to the viscosity data determined at laboratory conditions with the fresh oil.

The lubricant film thickness significantly influences the micropitting and wear performance of gear applications and, to a smaller extent, it also affects the pitting and scuffing performance. Knowledge of the actual lubricant film thickness in a gear contact is therefore essential for a reliable estimation of the failure risks of wear and micropitting, which are recently more and more the focus of interest.

For that reason, the efficiency of viscosity index (VI) improvers in EHL contacts was investigated by systematic measurements of the lubricant film thickness. Various types of polymers with various molecular weights and concentrations in the base oil were included in the test program in order to determine the influence of each parameter on the formation of lubricant films separately from each other.

Test Lubricants

The investigations were carried out with more than 20 test lubricants, which were blended especially for this research project. The base oils were two straight-paraffin-base mineral oils, M32 and M100, of the viscosity grades ISO VG 32 and ISO VG 100. The polymers that were used consisted of PMA (polyalkylmethacrylate), PIB (polyisobutylene), OCP (olefin copolymer), SBC (styrene butadiene copolymer) and STAR (star-shaped styrene isoprene copolymer). For each type of those polymers, a set of five different blends was investigated, which is shown in Table 1 for the polymer PMA, as an example. Each polymer type was available with low molecular weight (designated by the codes PMA1, OCP1, etc.) and high molecular weight (PMA2, OCP2, etc.). The polymers with low molecular weight were added in low concentration (PMA1L, OCP1L, etc.) and high concentration (PMA1H, OCP1H, etc.) to the base oil M100 and in very high concentration to the base oil M32 (PMA1VH, OCP1VH, etc.). The polymers with high molecular weight were added in low concentration to base oil M100 (PMA2L, OCP2L, etc.) and in high concentration to base oil M32 (PMA2H, OCP2H, etc.).

The polymer concentration in each blend was chosen with respect to equal kinematic viscosities ν_{100} of all test lubricants at 100°C, so that the lubricant film thicknesses of all oils could be directly compared at high temperature. Emphasis was put on higher-viscous blends (ν_{100} = 20 mm²/s), in order to get measurable film thicknesses at high temperatures up to 110°C, at which the investigations were performed. For a direct comparison with a straight mineral oil, a straight-paraffin-base mineral oil M240 with the same kinematic viscosity of ν_{100} = 20 mm²/s at 100°C was included in the set of test lubricants.

Table 1–Systematics of test lubricants for PMA-containing oils as examples.

Code of test oil	Molecular weight		Concentration			Base oil		Viscosity ν_{100} in mm²/s	
	low	high	low	high	very high	M32	M100	12.6	20
PMA1L	X		X				X	X	
PMA1H	X			X			X		X
PMA2L		X	X				X		X
PMA2H		X		X		X			X
PMA1VH	X				X	X			X

The investigation of a set of five different blends, as shown in Table 1 for each type of polymers, gives information about:

- the influence of the concentration of polymers with the same molecular weight in the same base oil (PMA1L and PMA1H),
- the influence of the molecular weight of the polymers in blends with the same viscosity at 100°C and with the same base oil, and
- the influence of the base oil viscosity in blends with the same polymer type (low and high molecular weight) and with the same viscosity at 100°C.

The STAR-type polymers were investigated in two blends only, which were equivalent to the blends with high molecular weight (…2L, …2H).

Shear Stability of Investigated Polymers

Permanent Viscosity Loss. Polymer-containing oils can suffer a permanent viscosity loss when being subject to mechanical loads, which can shred the polymer chains. That process is not reversible.

All polymer-containing test oils were subjected to a 20-hour tapered-roller-bearing shear test (KRL-shear test) according to CEC L-45-A-99 (Ref. 2), in order to determine the permanent viscosity loss by shearing. In this test, a tapered roller bearing 32008XQ is lubricated

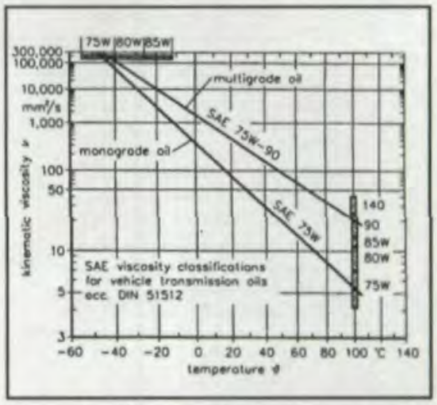

Figure 1—Difference between monograde and multigrade gear oils for vehicles.

Professor Dr.-Ing. Bernd-Robert Höhn
is head of the Institute of Machine Elements and the Gear Research Centre, both at the Technical University of Munich, Germany. The centre performs basic and applied research in the fields of load-carrying capacity and tribology of gears and automotive components.

Professor Dr.-Ing. Klaus Michaelis
is research group manager at the Gear Research Centre. He is responsible for experimental elastohydrodynamics and tribology and their application to gear scuffing and wear phenomena.

Dr.-Ing. Franz Kopatsch
is head of the calculation group at Steinbock GmbH, a German manufacturer of electric forklift trucks. A mechanical engineer, he worked from 1994 to 2000 as a scientific assistant at the Gear Research Centre. As an assistant, he performed two research projects on the influence of viscosity-index improvers on EHL-film thickness.

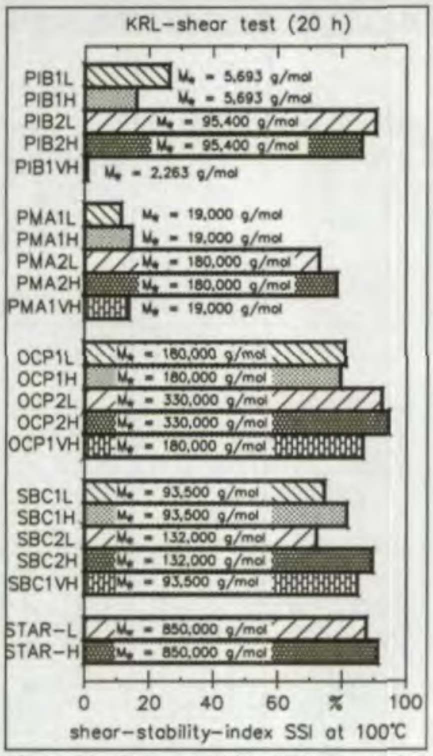

Figure 2—Shear stability indices of the test oils after a KRL-shear test.

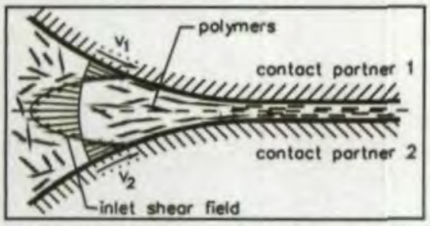

Figure 3—Arrangement of polymers in the inlet shear field of an EHL contact.

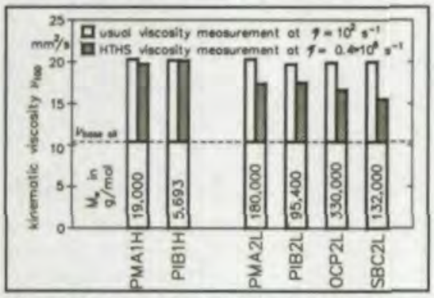

Figure 4—Results of HTHS viscosity measurements.

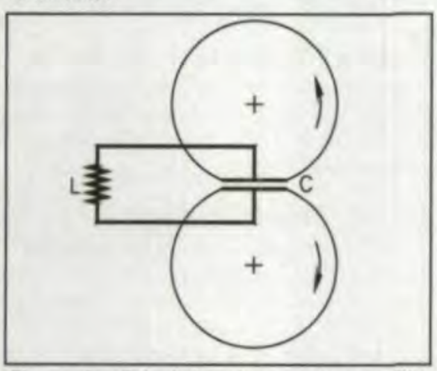

Figure 5—Principle of capacitance film thickness test method.

with 40 ml of the test fluid by dip lubrication at 60°C. The bearing is run for 20 hours at 1,450 rpm and at a load of 5 kN. The kinematic viscosity ν_{100} of the test oil is measured before and after the test at 100°C. With this information and the viscosity of the base oil $\nu_{100,base\ oil}$, the shear stability index (*SSI*) of the polymer in the blend can be calculated. It is defined as:

$$SSI = \frac{(\nu_{100,fresh} - \nu_{100,KRL})}{(\nu_{100,fresh} - \nu_{100,base\ oil})} \qquad (1)$$

with

$\nu_{100,fresh}$ = kinematic viscosity in mm²/s of the fresh polymer-containing oil, determined at a temperature of 100°C by using a capillary viscometer,

$\nu_{100,KRL}$ = kinematic viscosity in mm²/s of the polymer-containing oil after a KRL-shear test according to CEC L-45-A-99 (Ref. 2), determined at a temperature of 100°C by using a capillary viscometer, and

$\nu_{100,base\ oil}$ = kinematic viscosity in mm²/s of the base oil, determined at a temperature of 100°C by using a capillary viscometer.

The shear-stability index is an indicator for the shear-stability of the polymers. *SSI* = 0% means that the polymer-containing oil has the same viscosity after the KRL-shear test as before, so the polymers are shear-stable. SSI = 100% means that the polymer-containing oil has only the viscosity of the base oil after the KRL-shear test, so the viscosity-increasing effect of the polymers has completely disappeared after the test. In this case, the polymers are unstable against shear.

The shear-stability indices of the polymer-containing oils, which were derived from the KRL-shear tests, are shown in Figure 2. The shear-stability strongly depends on the average molecular weight of the polymers. For example, the test oils containing the polymers PIB1 and PMA1, which have a molecular weight M_w of less than 20,000 g/mole each, show the lowest shear-stability indices after the KRL-shear test, so those polymers are relatively stable against permanent shearing. All of the other polymers that were investigated have molecular weights M_w of more than 90,000 g/mole at fresh-oil condition. The shear-stability indices of the corresponding oils are all more than 70%. That means that after the KRL-shear test, the polymer chains are broken into pieces and hardly able to significantly increase the blend viscosity above the base oil viscosity.

Temporary Viscosity Loss

Long-stretched polymer chains tend to arrange themselves in parallel within a shear field, as shown in Figure 3. That way, the probability of the polymers becoming tangled with each other is reduced and so is the thickening effect of the polymers. This process is reversible. Such a shear field exists in the inlet region of any oil-lubricated EHL contact. It is caused by the back-flow of the surplus oil.

To get information about the temporary viscosity loss, high-temperature-high-shear (HTHS) viscosity measurements were carried out with some of the test oils. A capillary viscometer aided by air pressure was used to increase the velocity of the oils flowing through the capillary. That way, the shear ratio of the oil in the capillary could be increased from $\gamma \approx 10^2\ s^{-1}$ at pure-gravity-induced flow to some $0.4 \cdot 10^6\ s^{-1}$ at air-pressure-aided flow.

The results of the HTHS viscosity measurements are shown in Figure 4 for the oils PMA1H, PIB1H, PMA2L, PIB2L, OCP2L and SBC2L. The temporary viscosity loss of the oils containing long-chain polymers is significantly higher than that of the oils containing short-chain ones. The SBC polymers appear to be especially susceptible to temporary viscosity loss, as they lose about half of their thickening power at the high shear ratio in Figure 4.

Results of Film Thickness Measurements

Test Principle. The measurements were carried out in a twin-disk test rig. The core of the test rig consists of two cylindrical steel disks, each one 80 mm in diameter. They can be driven separately from each other with continuously variable speeds and can be loaded with a normal force F_N. The test oil is injected between both disks. The bulk temperatures ϑ_1 and ϑ_2 of both disks are measured with temperature sensors in boreholes 2 mm below the running surfaces. A detailed description of the test rig and of the test disks is given in Reference 9.

When loaded and thus elastically deformed, both disks and the lubricant between them form a capacitor (see Fig. 5), the capacitance C of which depends on the lubricant film thickness h_{meas}, the relative dielectric coefficient ε_{oil} of the lubricant, the deformed Hertzian contact width b and the disk width l_{eff} according to Equation 2.

$$C = \varepsilon_0 \cdot \varepsilon_{oil} \cdot (A/h_{meas})$$
$$\text{with } A = 2 \cdot b \cdot l_{eff} \qquad (2)$$

The "disk capacitor" is integrated into a resonance circuit, the frequency f of which depends on the capacitance C and a known inductivity L. By using a capacitance-frequency-calibration curve, the capacitance C can be derived from the resonance circuit's frequency f, which is determined by using a frequency counter.

The relative dielectric coefficient of the oil ε_{oil} is measured in a high pressure cell as a function of pressure and temperature. The deformed Hertzian contact width b can be calculated with the Hertzian equations. With that data, the lubricant film thickness h_{meas} of the oil can be calculated from the capacitance C of the disk capacitor by numerical integration. The calculation method used is based on Equation 2. It divides the contact zone into five separate sections with different portions of the entire capacitance and also takes into account the influence of an insulating layer made from Al_2O_3, which is applied to one of the disk surfaces by ion beam sputtering in order to prevent electric shortcuts between the disks. More detailed information about the measuring technique used is given in Reference 13.

Film Thickness of Polymer-Containing Oils. In the following, the most important results of the film thickness measurements of the test oil blends ...1H and ...2L (see Table 1) are presented. A detailed description and discussion of all test results gained in this project can be found in Reference 9.

The viscosity-temperature curves of the blends ...1H and ...2L are shown in Figures 6 and 7. All polymer-containing test oils were blended with equal kinematic viscosities at 100°C of $\nu_{100} = 20$ mm²/s, which is the value of the reference mineral oil M240. The base oil M100 has a kinematic viscosity at 100°C of approximately 10 mm²/s.

Figure 8 shows the measured film thicknesses of the test oils with polymers having low molecular weight and high concentration (PIB1H, OCP1H, SBC1H, PMA1H) and of the straight mineral oils M100 and M240 plotted against the bulk temperature ϑ_M of the disks. $\vartheta_M = (\vartheta_1 + \vartheta_2)/2$ is the average measured bulk temperature of both disks. At high temperatures, the oils PIB1H and PMA1H form film thicknesses similar to the mineral oil M240, which has the same kinematic vis-

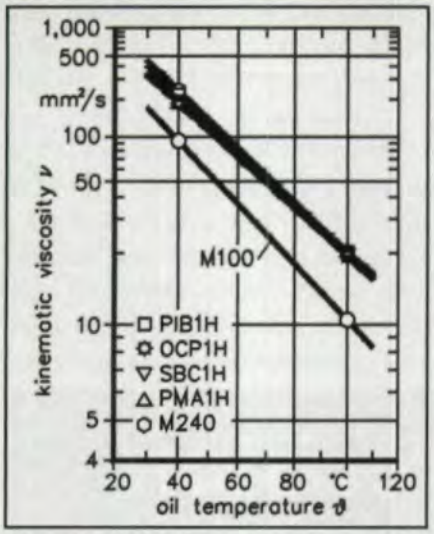

Figure 6—Viscosity temperature curves of test oils …1H.

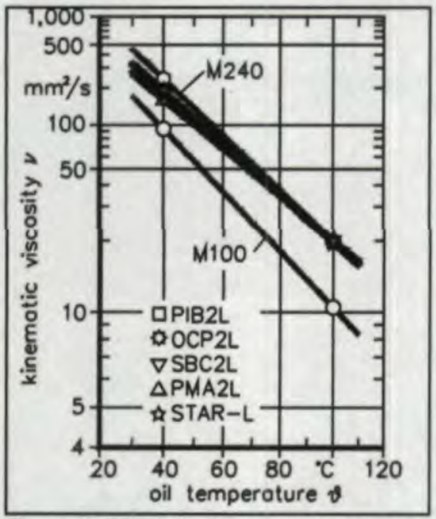

Figure 7—Viscosity temperature curves of test oils … 2L.

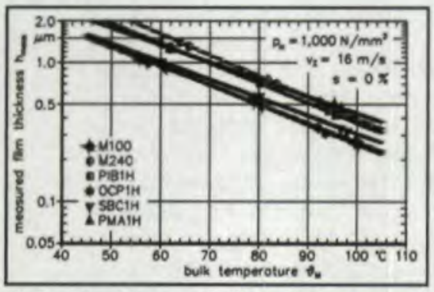

Figure 8—Measured film thicknesses of test oils … 1H.

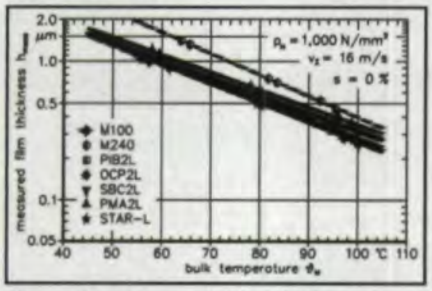

Figure 9—Measured film thicknesses of test oils … 2L.

cosity v_{100} as the polymer-containing oils. At low temperatures, however, the film thicknesses of PIB1H and PMA1H are lower than those of M240. The VI-improving effect of the polymers PIB1 and PMA1 can be seen quite clearly here.

On the other hand, the oils OCP1H and SBC1H show only very little increase of the film thickness compared to the base oil M100. Within the accuracy of measurement, the oil OCP1H doesn't even show an increase of the film thickness compared to M100 at all. That is a consequence of the ability of the polymers SBC and OCP to form physical and chemical network structures. Those networks have a high thickening effect at standard conditions. At high pressure, temperature and shear rate, as in an EHL contact, however, those network structures are obviously not very stable and therefore lose a great part of their thickening power.

Figure 9 shows the measured film thicknesses of the test oils with polymers of high molecular weight and low concentration PIB2L, OCP2L, SBC2L, PMA2L, STAR-L and of the two mineral oils M100 and M240 at the same conditions as in Figure 8. None of the polymer-containing oils reaches the film thicknesses of the mineral oil M240 despite equal kinematic viscosities v_{100}. That is a consequence of the high molecular weight of those polymers, which causes a high temporary viscosity loss under the influence of a shear field, as shown in Figure 3. As the viscosity of an oil in the inlet region of an EHL contact is decisive for the height of the film thickness and as the viscosities of the test oils containing long-chain polymers are reduced to some extent within the high shear field in the inlet region of the disk contact, those test oils form lower film thicknesses than expected according to their viscosity data gained at standard laboratory conditions.

Film Thickness Calculation

Film Thickness Calculation in General. The lubricant film thicknesses h_{min} according to Dowson/Higginson (Ref. 5) and h_0 according to Ertel/Grubin (Refs. 6 and 8) in an EHL contact can be calculated for line contact condition as follows:

$$h_{min} = 2.65 \cdot R \cdot G^{0.54} \cdot U^{0.7} \cdot W^{-0.13} \qquad (3)$$

$$h_0 = 1.95 \cdot R \cdot (G \cdot U)^{0.73} \cdot W^{-0.09} \qquad (4)$$

The nondimensional EHL parameters G, U and W in the above equations are defined as:

$$G = \alpha \cdot E' \qquad (5)$$

$$U = (\eta_M \cdot v_\Sigma)/(2 \cdot R \cdot E') \qquad (6)$$

$$W = 2 \cdot \pi \cdot [(p_H/E')^2] \qquad (7)$$

The reduced Young's modulus E' and the reduced radius of curvature R are calculated as follows:

$$E' = 2[(1\text{-}v_1^2/E_1) + (1\text{-}v_2^2/E_2)]^{-1} \qquad (8)$$

$$R = (r_1 \cdot r_2)/(r_1 + r_2) \qquad (9)$$

According to Murch/Wilson (Ref. 12), the accuracy of film thickness calculation can be improved by thermal correction, which takes into account the temperature rise of the oil in the inlet region of the contact, the rise being caused by the backflow of the surplus oil.

$$h_{min,\, thermal} = h_{min} \cdot C \qquad (10)$$

$$h_{0,\, thermal} = h_0 \cdot C \qquad (11)$$

with

$$C = 3.94/(3.94 + L^{0.62}) \qquad (12)$$

$$L = (\eta_M \cdot \alpha_t \cdot v_\Sigma^2)/(4 \cdot \lambda) \qquad (13)$$

$$\alpha_t = \ln(\eta_{40°C}/\eta_{100°C})/60K \qquad (14)$$

Modification of Film Thickness Calculation for Polymer-Containing Oils. As the film thickness measurements prove, polymer-containing oils hardly ever form film thicknesses as high as a straight mineral oil of equal viscosity. That means that the usual kinematic viscosity, which is determined in a capillary viscometer at standard conditions, is not sufficient as an indicator for the film thicknesses to be expected for polymer-containing oils. As the usual film thickness calculation methods according to Dowson/Higginson (Ref. 5) or Ertel/Grubin (Refs. 6 and 8) include only the standard laboratory viscosity data, deviations between calculated and actual film thicknesses cannot be avoided for polymer-containing oils.

An improvement of the accuracy of film thickness calculation for polymer-containing oils requires modifying the calculation equations with a factor that correctly reflects the effective viscosity increase of polymers in an EHL contact. Polymer-specific properties, such as type, concentration or molecular weight of the polymers, cannot be used for such a factor, because those properties are usually not available to the user.

So a nondimensional polymer-correction factor P was derived from the film thickness test results. The factor takes into account the viscosity loss of a polymer-containing oil after a KRL-shear test. This term seems to be apt to specify the efficiency of polymers in an EHL contact, as the measurements showed a good correlation of high viscosity losses after a KRL-shear test with poor film thickness performance and vice versa. Besides, the KRL-shear test is a common and simple test method and its test devices are available in many laboratories.

The polymer-correction factor, which was derived from the test results, is defined as:

$$P = (\nu_{100,\,KRL} / \nu_{100,\,fresh})^{0.7} \qquad (15)$$

The exponent 0.7 in the above equation was chosen with respect to the weighting of the dynamic viscosity η in the usual film thickness equations.

The polymer-correction factor P is used to calculate the film thickness of polymer-containing oils as follows:

$$h_{min,\,thermal,\,pol.} = h_{min,\,thermal} \cdot P \qquad (16)$$

$$h_{0,\,thermal,\,pol.} = h_{0,\,thermal} \cdot P \qquad (17)$$

Those equations can, of course, also be used to calculate the film thickness of straight mineral or synthetic oils. In this case, the polymer-correction factor equals 1, because polymer-free oils practically don't lose any viscosity during a KRL-shear test. So the correction factor P is universally applicable for all lubricating oils.

The improvement of the accuracy of film thickness calculation by using the polymer-correction factor P is shown in Figures 10–13.

In Figure 10, the film thicknesses $h_{0,thermal}$, which were calculated without the polymer-correction factor P, are plotted against the measured film thickness-

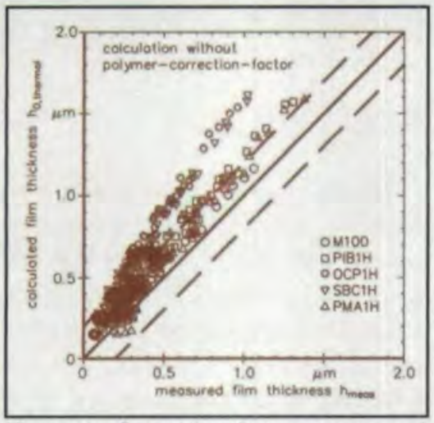

Figure 10—Comparison between measured and calculated film thicknesses of test oils ... 1H without polymer-correction factor.

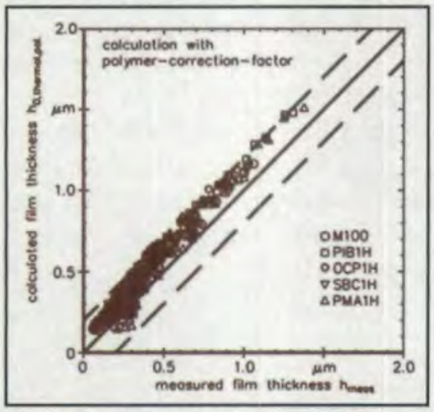

Figure 11—Comparison between measured and calculated film thicknesses of test oils ... 1H with polymer-correction factor.

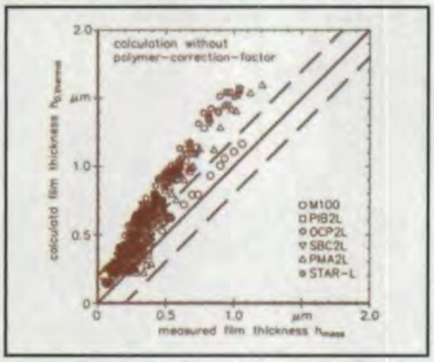

Figure 12—Comparison between measured and calculated film thicknesses of test oils ... 2L without polymer-correction factor.

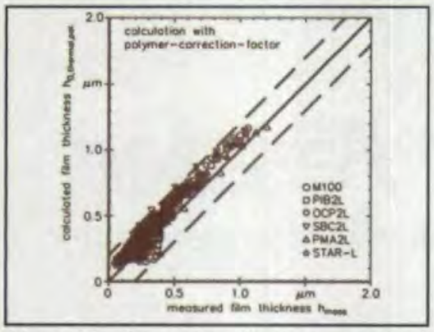

Figure 13—Comparison between measured and calculated film thicknesses of test oils ... 2L with polymer-correction factor.

es h_{meas} of the test oils ...1H. All film thickness measurements at all conditions that had been carried out were regarded. The calculation overestimates the film thicknesses of the polymer-containing oils, especially those of SBC1H and OCP1H. For the polymer-free base oil M100, there is already a good correlation between measured and calculated film thicknesses. When modifying the calculation with the polymer-correction factor *P*, the accuracy of film thickness prediction improves considerably, as can be seen in Figure 11, where measured and calculated film thicknesses correlate quite well within the marked scatter range of ± 0.2 µm, even for the polymer-containing oils. For the majority of the measurements, the calculated film thicknesses are still slightly higher than the measured ones. That is a consequence of the difference between the bulk temperature ϑ_M,which is measured 2 mm below the disk surfaces and used for film thickness calculation, and the actual—slightly higher—temperature in the inlet region of the EHL contact. So the actual viscosity in the inlet region of the contact and thus also the actual film thickness are slightly lower than calculated.

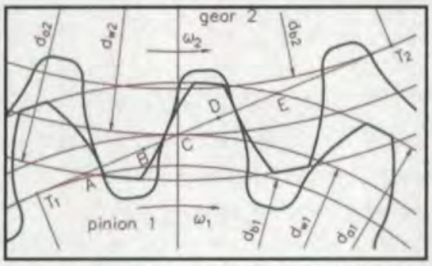

Figure 14—Line of contact of C-PT-type gears.

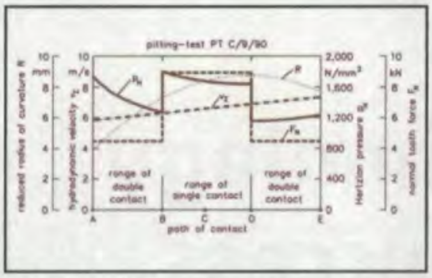

Figure 15—Some gear-specific parameters along the path of contact.

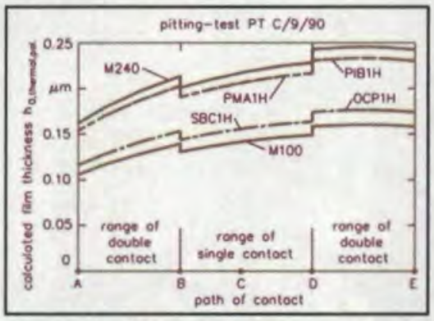

Figure 16—Calculated film thicknesses of test oils ... 1H at pitting-test conditions.

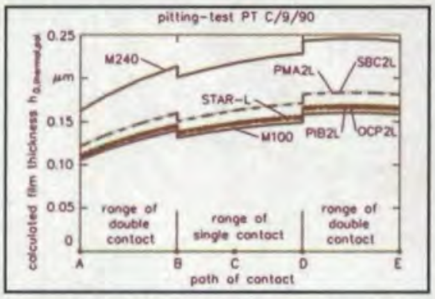

Figure 17—Calculated film thicknesses of test oils ...2L at pitting-test conditions.

The use of applying the polymer-correction factor *P* to film thickness calculation for oils containing long-chain polymers is shown in Figures 12 and 13. The test oils ...2L with long-chain polymers suffer from a high temporary and permanent viscosity loss by shearing. Using the polymer-correction factor *P* leads to a considerable improvement of the accuracy of film thickness calculation for the polymer-containing oils.

Altogether, the proper applicability of the polymer-correction factor *P* has been checked with approximately 3,000 film thickness measurements with 32 different polymer-containing oils, and it provided good results.

Application of the Modified Film Thickness Calculation to Gear Contacts. Figure 14 shows the line of contact of a C-PT-type spur gear pair as it is used for the standard pitting test PT C/9/90 (Ref. 7). Pinion 1 has 16 teeth, gear 2 has 24 teeth and the module is 4.5 mm. The base circles d_{b1} and d_{b2}, the pitch circles d_{w1} and d_{w2} and the tip circles d_{a1} and d_{a2} are shown in Figure 14 as well. The path of contact is limited on the line of contact by the beginning A and end E of contact. The points B and D represent the beginning and end of the range of single contact. C is the pitch point. The line of contact touches the base circles in points T_1 and T_2.

For calculating the lubricant film thickness within a gear contact, the distributions of the reduced radius of curvature R, the hydrodynamic velocity v_Σ and the Hertzian pressure p_H along the path of contact need to be known. As an example, those parameters are shown in Figure 15 for a C-PT-type gear pair and for the conditions of the standard pitting-test PT C/9/90. The reduced radius of curvature R forms a parabola along the line of contact, which equals 0 in T_1 and T_2. The hydrodynamic velocity v_Σ increases linearly from A to E. For the calculation of the Hertzian contact pressure, the normal tooth force F_N was assumed to be 100% in the range of single contact and to be 50% in the range of double-tooth contact. That is a simplification, which does not consider dynamic tooth forces. If the course of dynamic tooth forces along the path of contact is known by measurement or by calculation, the Hertzian contact pressure can be calculated more accurately.

With that gear data, the film thickness can be calculated along the path of contact of a gear mesh. An example is shown in Figure 16. The film thickness $h_{0,thermal,pol.}$, which was calculated according to Ertel/Grubin (Refs. 6 and 8), with thermal correction according to Murch/Wilson (Ref. 12) and polymer-correction factor P, is plotted against the path of contact of a C-PT-type gear pair for the conditions of the standard pitting-test PT C/9/90 for the test oils with short-chain polymers and high concentrations. The relevant tooth bulk temperature was assumed to be constant at 100°C. Without using the polymer-correction factor P, the film thicknesses of all polymer-containing oils would be calculated equal to that of M240. Using the polymer-correction factor P, the calculated film thicknesses of the polymer-containing oils represent the actually measured values better (see Fig. 8).

Another calculation example in Figure 17 shows the film thicknesses of the test oils …2L with the long-chain polymers in low concentration. Again, calculation would provide film thicknesses equal to M240 for all polymer-containing oils without using the polymer-correction factor. With the factor, the calculated film thicknesses show much better correlation with the measured ones (see Fig. 9).

Summary

The lubricant film thicknesses of a number of polymer-containing oils and their base oils were measured systematically in a twin-disk test rig. The investigated polymers were polyalkylmethacrylates (PMA), polyisobutylenes (PIB), olefin copolymers (OCP), styrene butadiene copolymers (SBC) and star-shaped styrene isoprene copolymers (STAR), each with two different molecular weights. In addition, the base oil viscosity and the concentration of the polymers in the base oil were varied. For information about the shear-stability of the polymers, the temporary and permanent viscosity loss by shearing were determined separately from each other by means of HTHS-viscosity measurements and KRL-shear-stability tests.

All polymer-containing oils formed lower film thicknesses than a straight mineral oil of the same kinematic viscosity v_{100} over a wide range of operating conditions. Short-chain polymers in high concentration in the base oil turned out to be significantly more effective in the contact than long-chain polymers in low concentration with the same viscosities. Polymers with thickening power mainly based on the formation of network structures, such as SBC, provided poor film forming properties. Those findings are in good accordance with the findings of other authors, for instance Professor Spikes (Refs. 11, 14 and 15) from the Imperial College in London, who carried out a great number of optical film thickness measurements with various polymer-containing oils.

A correction factor *P* was derived from the test results, by which the accuracy of film thickness calculation can be improved significantly for polymer-containing oils. The application of the correction factor is demonstrated and its practical use is exemplified by calculating the film thicknesses of some polymer-containing oils in a gear contact.

Acknowledgments

This research project was sponsored by the German Society for Petroleum and Coal Science and Technology (DGMK) in the German Federation of Industrial Cooperative Research Associations (AiF) by funds of the German Federal Ministry of Economics and Technology (BMWi). ○

References

1. Bartz, W.-J. "Bewertung des reversiblen und irreversiblen Viskositätsverlustes von Mehrbereichsölen," *Tribologie und Schmierungstechnik*, 41. Jahrgang, 4/1994, S. 214–218.

2. CEC L-45-A-99, "Viscosity Shear Stability Test Procedure for the Tapered Roller Bearing Test Rig," 1999.

3. CEC L-37-T-85, "Shear Stability of Polymer-Containing Oils (FZG Spur Gear Test Rig)," 1986.

4. DIN/ISO 2909, "Berechnung des Viskositätsindex aus der kinematischen Viskosität," July 1979.

5. Dowson, D. and G.R. Higginson, *Elastohydrodynamic Lubrication*, Oxford. Pergamon Press, 1966.

6. Ertel-Mohrenstein, A. "Die Berechnung der hydrodynamischen Schmierung gekrümmter Oberflächen unter hoher Belastung und Relativbewegung," *VDI-Fortschrittsbericht* Reihe 1, Nr. 115, 1984.

7. *FVA-Informationsblatt* zum Forschungsvorhaben Nr. 2/IV: "Pittingtest – Einfluß des Schmierstoffes auf die Grübchenlebensdauer einsatzgehärteter Zahnräder im Einstufen- und im Lastkollektivversuch," 1997.

8. Grubin, A.N. and J.E. Vinogradova, *Investigation of the contact machine components*, Cent. Sci. Res. Inst. Tech. Mech. Eng., Moscow, Book No. 30, 1949.

9. Kopatsch, F. "Systematische Unter-suchungen zum Einfluß von polymeren Zusätzen auf die EHD-Schmierfilmdicke," *DGMK-Forschungsbericht* Nr. 466-01, 1999.

10. Mann, U. "Messung von Schmierfilmdicken im EHD-Kontakt. Einfluß verschiedener Grundöle und Viskositäts-Index-Verbesserer," *DGMK-Forschungsbericht* Nr. 466, 1995.

11. Mitsui, H. and H.A. Spikes, "Predicting EHD Film Thickness of Lubricant Polymer Solutions," *Tribology Transactions*, Vol. 41, 1, 1998, pp. 1–10.

12. Murch, L.E. and W.R.D. Wilson, "A Thermal Elastohydrodynamic Inlet Zone Analysis," *Trans. ASME F. J. Lubr. Techn.* 97, 2, 1975, pp. 212–216.

13. Simon, M. *Messung von elasto-hydrodynamischen Parametern und ihre Auswirkung auf die Grübchentragfähigkeit vergüteter Scheiben und Zahnräder*, Diss. TU München, 1984.

14. Smeeth, M., H.A. Spikes and S. Gunsel, "The Formation of Viscous Surface Films by Polymer Solutions: Boundary or Elastohydrodynamic Lubrication?" *Tribology Transactions*, Vol. 39, 3, 1996, pp. 720–725.

15. Smeeth, M., H.A. Spikes and S. Gunsel, "Boundary Film Formation by Viscosity Index Improvers," *Tribology Transactions*, Vol. 39, 3, 1996, pp. 726–734.

Tell Us What You Think . . .

If you found this article of interest and/or useful, please **circle 312.**

If you did not care for this article, **circle 313.**

If you would like to respond to this or any other article in this edition of Gear Technology, please fax your response to the attention of Randy Stott, managing editor, at 847-437-6618 or send e-mail messages to *people@geartechnology.com.*

U.S. Postal Service Statement of Ownership, Management and Circulation As of September 30, 2001

Publication Title: Gear Technology, The Journal of Gear Manufacturing
ISSN No.: 0743-6858
Published: Bimonthly, 6 issues per year
Annual Subscription Price: $45.00
Mailing Address of Publication: 1425 Lunt Avenue, Elk Grove Village, Cook County, IL 60007
Name & Mailing Address of Publisher: Michael Goldstein, 1425 Lunt Avenue, Elk Grove Village, Cook County, IL 60007
Name & Mailing Address of Editor: Michael Goldstein, 1425 Lunt Avenue, Elk Grove Village, Cook County, IL 60007
Name & Mailing Address of Managing Editor: Michael Goldstein, 1425 Lunt Avenue, Elk Grove Village, Cook County, IL 60007
Name & Mailing Address of Owner: Michael Goldstein & Richard Goldstein, 1425 Lunt Avenue, Elk Grove Village, Cook County, IL 60007
Known Bondholders: None

Issue Date for Circulation Data Below: September/October 2001

Extent and Nature of Circulation	Actual No. Copies of Single Issue Published Nearest to Filing Date	Average No. Copies Each Issue During Preceding 12 Months
a. Total Number of Copies (Net press run)	14,482	14,036
b1. Paid/Requested Outside-County Mail Subscriptions, as Stated on Form 3541	9,527	9,467
b2. Paid In-County Subscriptions, as Stated on Form 3541	0	0
b3. Sales Through Dealers and Carriers, Street Vendors, Counter Sales and Other Non-USPS Paid Distribution	350	346
b4. Other Classes Mailed Through the USPS	0	0
c. Total Paid and/or Requested Circulation	9,877	9,813
d1. Free Distribution Outside-County, as Stated on Form 3541	2,551	1,470
d2. Free Distribution In-County, as Stated on Form 3541	0	0
d3. Free Distribution Other Classes Mailed Through the USPS	0	0
e. Free Distribution Outside the Mail	1,322	1,613
f. Total Free Distribution	3,873	3,083
g. Total Distribution	13,750	12,896
h. Copies Not Distributed	732	1,140
i. Total	14,482	14,036
j. Percent Paid and/or Requested Circulation	71.8%	76.1%